Microstructure and strain analysis of GaN epitaxial films using in-plane grazing incidence x-ray diffraction*

Guo Xi(郭 希)[a)†], Wang Yu-Tian(王玉田)[a)], Zhao De-Gang(赵德刚)[a)], Jiang De-Sheng(江德生)[a)], Zhu Jian-Jun(朱建军)[a)], Liu Zong-Shun(刘宗顺)[a)], Wang Hui(王 辉)[a)], Zhang Shu-Ming(张书明)[a)], Qiu Yong-Xin(邱永鑫)[b)], Xu Ke(徐 科)[b)], and Yang Hui(杨 辉)[a)b)]

[a)] *State Key Laboratory on Integrated Optoelectronics, Institute of Semiconductors, Chinese Academy of Sciences, Beijing* 100083, *China*

[b)] *Suzhou Institute of Nano-tech and Nano-bionics, Chinese Academy of Sciences, Suzhou* 215125, *China*

(Received 17 September 2009; revised manuscript received 23 December 2009)

This paper investigates the major structural parameters, such as crystal quality and strain state of (001)-oriented GaN thin films grown on sapphire substrates by metalorganic chemical vapour deposition, using an in-plane grazing incidence x-ray diffraction technique. The results are analysed and compared with a complementary out-of-plane x-ray diffraction technique. The twist of the GaN mosaic structure is determined through the direct grazing incidence measurement of (100) reflection which agrees well with the result obtained by extrapolation method. The method for directly determining the in-plane lattice parameters of the GaN layers is also presented. Combined with the biaxial strain model, it derives the lattice parameters corresponding to fully relaxed GaN films. The GaN epilayers show an increasing residual compressive stress with increasing layer thickness when the two dimensional growth stage is established, reaching to a maximum level of –0.89 GPa.

Keywords: in-plane grazing incidence x-ray diffraction, gallium nitride, mosaic structure, biaxial strain

PACC: 6855, 7870C, 7280E

1. Introduction

GaN-based semiconductors have shown to be promising materials in applications of wide variety of optoelectronic and electronic devices such as blue/ultraviolet light-emitting diodes, laser diodes as well as high power, frequency and temperature devices.[1−4] Due to the lack of native bulk GaN substrates, heteroepitaxial GaN films usually are grown on foreign substrates, for instance, on sapphire or silicon carbide substrates in commercial application. Epitaxial GaN films are characterised as mosaic structures which exhibit a high density of threading dislocations originating from the large lattice mismatch and thermal expansion coefficient mismatch to the substrates.[5] The dislocations play a significant role in leakage current, yellow photoluminescence and non-radioactive combination which strongly limit the efficiency and lifetime of the devices.[6−8] Despite of the presence of strain-relieving threading dislocations, GaN heteroepitaxial films are normally under significant residual strain. The strain is often linked to bending or cracking of epitaxial films[9] and poses issues for device processing such as facet cleavage and photolithography. Furthermore it has impact on electronic band structures and luminescence properties.[10] The light emission wavelength of InGaN/GaN multi-quantum-wells can be adjusted by strain fields.[11] The strain can also act as a driving force for formation and evolvement of structure defects.[12] At present, the epitaxial growth of GaN thin films with high crystallographic quality still remains a key issue for the fabrication and performance of GaN-based devices.

The x-ray technique provides essential tool for structural investigation of distorted and defective crystals. In comparison with other methods, such as transmission electron microscopy (TEM), x-ray diffraction (XRD) method has the advantage of being convenient and non-destructive as well as giving averaged information on a large scale region. Another prominent advantage of the x-ray method is the high sensitivity to strain with a resolution of ppm level

*Project supported by the National Natural Science Foundation of China (Grant Nos. 60506001, 60776047, 60976045 and 60836003), the National Basic Research Programme of China (Grant No. 2007CB936700) and the National Science Foundation for Distinguished Young Scholars, China (Grant No. 60925017).

†Corresponding author. E-mail: guox@semi.ac.cn

© 2010 Chinese Physical Society and IOP Publishing Ltd

and it is particularly applicable to evaluate strain distribution and lattice parameter in the epitaxial film system.[13] Conventional x-ray Bragg diffraction describes the structural properties perpendicular to the wafer surface or inclined at an angle to it. However structural information parallel to the wafer surface cannot be directly measured. In hexagonal wurtzite GaN-based epilayers, in-plane biaxial strain and a axis lattice parameter thus are normally extracted from out-of-plane measurements and calculations according to the elastic theory. The measurement processes involve a series of $(00l)$ symmetric reflections and (hkl) asymmetric reflections. In recent years, in-plane grazing incidence XRD has developed into a powerful technique for direct and efficient measurement of in-plane structure parameters owing to its intrinsic advantages. In this study, typical (001)-oriented GaN films were investigated with the in-plane diffraction function mode by a high resolution triple-axis x-ray diffractometer. The a axis lattice parameter was measured under in-plane scattering geometry together with the mosaic twist, and the stress state was checked based on the biaxial strain elastic model.

2. Experimental

The investigated (001)-oriented GaN films were grown by metal-organic chemical vapour phase epitaxy on c-plane sapphire substrate in a Thomas Swan Showerhead reactor. Trimethylgallium, ammonia (NH_3), and hydrogen (H_2) were used as Ga and N precursors and carrier gas, respectively. The conventional two-step growth method was adopted for the growth of GaN epilayers. First, an initial thin GaN buffer layer was deposited at 540 °C to accommodate the large lattice mismatch between GaN and sapphire. Then, the temperature was ramped up for the high temperature island growth followed by the transition from three dimensional (3D) to two dimensional (2D) growth mode and finally the growth of high quality GaN films was carried out at 1040 °C. The series of GaN epilayer samples investigated in this study were deposited under nominally identical condition but with different thickness (0.6, 0.8, 1.6 and 3.0 μm, respectively). These samples revealed variations in residual strain as will be discussed in detail later.

High resolution and in-plane grazing incidence XRD measurements were performed using Bruker D8 DISCOVER high-resolution x-ray diffractometer with a $CuK_{\alpha 1}$ target (λ = 1.54056 Å, 1 Å = 0.1 nm). A four-bounce Bartels Ge (220) crystal monochromator and a three-bounce Ge analyser crystal were applied for high-resolution configuration measurements. In grazing incidence geometry, x-ray tube was rotated 90° to enable an adjustable incidence angle with respect to the sample stage and the curved multilayer reflection optic (Göbel mirror) and double Soller Slit were employed to get the high intensity and low divergence angle incoming beam.

It is noted that the method of in-plane grazing incidence diffraction is especially suitable for studying very thin epitaxial films. It allows a direct access to lateral parameters such as lattice plane spacing and micro-strain. As the diffraction geometry illustrated in Fig. 1, the incident beam strikes the sample surface under a small glancing angle α_i which is close to the critical angle for total reflection α_c. It creates an evanescent wave with finite penetration depth. When we rotate the sample around the surface normal into the diffraction condition, the diffraction beam exits under a small glancing angle α_f with respect to the sample surface. Grazing incidence diffraction can be interpreted as a combination of diffraction at lattice planes perpendicular to the sample surface with reflection of the incident beam from the surface. Furthermore, the penetration depth of grazing incidence x-ray beam into sample changes as a function of incident angle α_i, which can be applied to characterise depth-dependent microstructure.

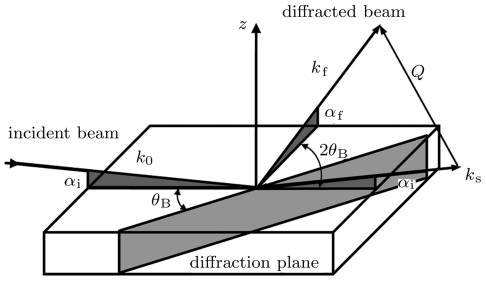


Fig. 1. Schematic illustration of in-plane grazing incidence diffraction geometry.

3. Results and discussion

The mosaic structure of heteroepitaxial GaN is described in terms of four crystallographic parameters: tilt, twist, lateral and vertical correlation lengths where tilt and lateral correlation lengths can be directly deduced from $(00l)$ on-axis ω scan with increasing reflection orders according to the Williamson–Hall

plot. The determination of in-plane orientation twist, however, shows considerably more difficulties. Based on a series of ω scans measured in skew symmetric geometry of diffraction planes with increasing inclined angle χ with respect to the basal plane, twist can be extracted from extrapolation when the inclined angle χ is reaching 90°.[14] We have performed ω-scan XRD rocking curve measurements on the 3 μm-thick sample for $(h0l)$ reflection as a function of interplanar angle χ shown in Fig. 2, where a least-squares fit to the full width at half maximum (FWHM) data is also presented. The extrapolation equation can be expressed as

$$\beta_{hkl}^2 = (\beta_{\text{tilt}} \cos\chi)^2 + (\beta_{\text{twist}} \sin\chi)^2, \qquad (1)$$

where β_{hkl} represents the ω-scan FWHM of the (hkl) reflection, β_{tilt} and β_{twist} are the mosaic tilt and twist spread respectively.

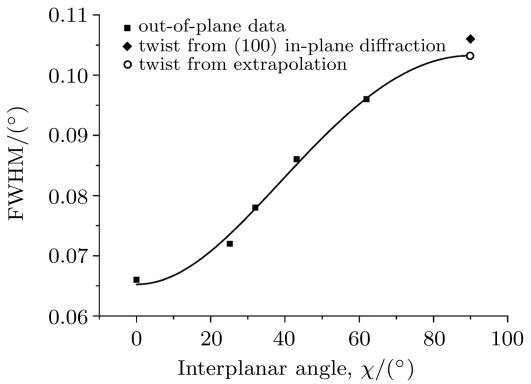


Fig. 2. The FWHM values of rocking curves for $(h0l)$ reflections as a function of interplanar angle between the reflecting lattice plane and the sample surface. The solid line is a least-squares fitting to the data according to Eq. (1). The extrapolated twist value agrees well with direct measurement value from (100) in-plane diffraction.

Alternatively, the grazing incidence in-plane diffraction provides a more efficient and simplified method to direct measure mosaic twist, which is discussed below. In Figs. 3(a) and 3(b), the Φ-scan and ω-scan diffraction profiles of GaN epilayer (100) reflection in grazing incidence are presented, respectively. In this case, it is noted that the ω-scan is more suitable for the determination of twist spread because the in-plane instrumental resolution of ω-scan reaches 0.0001° which is much superior to Φ-scan. In contrast, the crystallographic symmetry and phase composition can be characterized by Φ-scan owing to the full round scan range of 360° as the six fold symmetry in wurtzite GaN structure illustrated in Fig. 3(a). There are several kinds of potential broadening factors to be taken into account in the measured ω-scan FWHM (β_{m}) based on the broadening expression: $\beta_{\text{m}}^2 = \beta_0^2 + \beta_{\text{d}}^2 + \beta_{\text{t}}^2$, but the instrumental divergence (β_{d}, ~0.03°) and crystal intrinsic width (β_0) are comparatively small and can be neglected in comparison with the in-plane rotation (β_{t}). It is found that the measured curve can be well fitted to the Gaussian function, this result indicates that the FWHM is mainly induced by the mosaic twist β_{t}. To check the reliability of the result, we compare the direct measured FWHM value obtained from (100) in-plane diffraction with that obtained by the extrapolation method as shown in Fig. 2. It is found that the results of two methods agree with each other very well, this result confirms that the (100) ω-scan in grazing incidence can be effectively employed as the mosaic twist measurement.

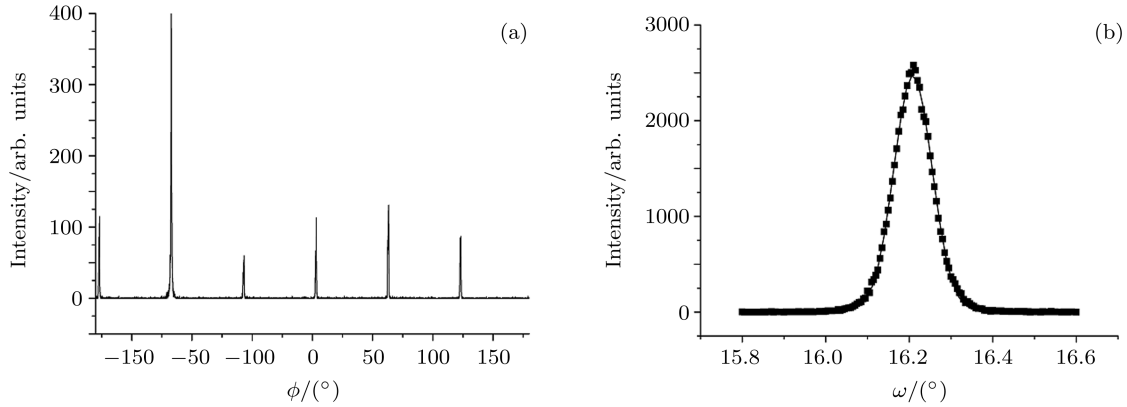


Fig. 3. (a) The (100) 360° Φ-scan and (b) (100) ω-scan grazing incidence diffraction of GaN epitaxial film in in-plane geometry as well as the Gaussian fit curve.

Figure 4(a) shows (100) in-plane rocking curves of GaN film measured at various grazing incident angle $\alpha_{\rm i}$ in order to investigate the dependence of crystalline quality distribution in the top GaN layer on film depth. When the grazing incident angle is less than the angle of total reflection,[15] the penetration depth of x-ray beam is calculated according to the following expression:

$$L \approx \frac{\lambda}{2\pi} \frac{1}{\left(\sqrt{\alpha_{\rm c}^2 - \sin^2 \alpha_{\rm i}}\right)}, \tag{2}$$

where λ is wavelength of the incident beam, $\alpha_{\rm i}$ and $\alpha_{\rm c}$ are incident and critical angle, respectively (see Fig. 1). If the grazing incident angle is larger than the angle of total reflection, the penetration depth of x-ray beam is approximately expressed as

$$L \approx \frac{1}{2\mu} \sin \alpha_{\rm i}, \tag{3}$$

where μ is linear absorption coefficient of GaN (429 cm^{-1}).[16] The calculated L values are ranging from 5 nm to 142 nm in this experiment depending on the value of $\alpha_{\rm i}$. As the result shown in the inset of Fig. 4(a), the FWHM values almost maintain unchanged when we increase the penetration depth of the probing beam demonstrating a homogeneous crystalline quality of the top GaN epilayer. The same tendency is also exhibited in Fig. 4(b) by performing ω–2θ scans of (100) reflection under the same experimental setup. This means that there is no remarkable depth-resolved variation in strain state in the top GaN layer within detectable region. Therefore, in this case the strain state can be determined by in-plane diffraction without concerning about its depth dependence. In addition, the error induced by sample horizontal alignment procedures will be small and may be neglected.

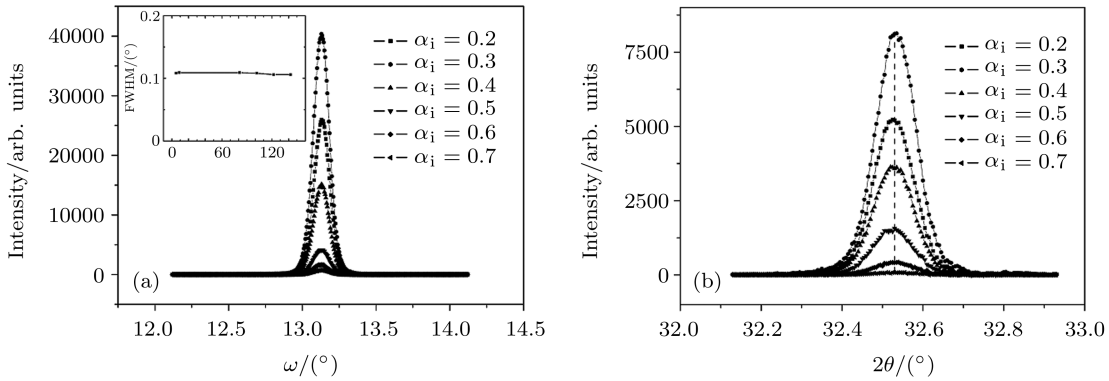


Fig. 4. (a) The (100) ω-scan grazing incidence reflection curves measured at different incident angle $\alpha_{\rm i}$. (b) The FWHM values for (100) reflections in dependence of incident angle $\alpha_{\rm i}$.

Normally, to determine the in-plane lattice parameter$a$ of the GaN film grown on sapphire, (00l) symmetric reflections are measured to directly obtain lattice parameter c at first. Then one or two asymmetric reflections of planes inclined with a large angle to the basal plane (such as (105) and (204)) are performed to evaluate interplanar spacing and then the average lattice parameter$a$ can be calculated. The calculation is based on the value of c and the following equation which depicts relation between different interplanar spacings:

$$\frac{1}{d_{hkl}^2} = \frac{4}{3} \frac{h^2 + k^2 + hk}{a^2} + \frac{l^2}{c^2}. \tag{4}$$

As a result, there are more inaccuracies found in a than c, owing to the fact that the error of a is increasing due to its dependence on the error of c value. Bond[17] and Fewster and Andrew[18] had advanced an improved method to measure the lattice parameters with high accuracy. In the Bond's technique, the $(n, -n)$ and the $(n, +n)$ of a single reflection are combined to remove the effect of the 'zero error'. According to Fewster's method the least-squares fitting procedures to Eq. (4) are carried out to obtain c and a simultaneously, and several correction effects are considered. However, when the thin film thickness is exceedingly small, the insufficient integrated diffraction

intensity and the peak profile broadening due to size effect make it difficult to enable an accurate measurement of the angular position of the diffraction curves. In contrast, the grazing incidence diffraction method is suitable for the measurement of the in-plane lattice parameter even for very thin films and it does not involve measuring out-of-plane lattice parameter beforehand. A relatively accurate in-plane lattice parameter measurement can be achieved by using lattice parameter of substrates as standard reference. However, the substrates are generally strained and curved during the high temperature growth and subsequently cooling down, so the unstrained native substrate lattice parameter value is less suitable to be taken as the reference. In addition, when the epilayer is thick enough (for example, being one micrometer or thicker), the reference substrate peak is too weak to detect due to the finite x-ray penetration depth in the grazing incidence geometry. Consequently, the in-plane lattice parameters of the top GaN epilayers are preferably determined on an absolute scale in this case.

Both (100) and (110) lattice planes of the (001) wurtzite GaN films show strong XRD characteristic peaks in the in-plane grazing incidence geometry. However, because the (220) reflection can not be achieved due to the limitation of instrumental range, only (100) high order reflections are performed in this study. When the angular positions of Φ and χ have been carefully calibrated, reflections from the same zone will satisfy Bragg's law $2d\sin\theta = n\lambda$ with its own $\theta_{\rm B} = \theta_{\rm m} + \Delta\theta$, where $\theta_{\rm m}$ is the measured reflection angle, $\Delta\theta$ is the Bragg angle correction due to zero setting. Therefore, we can deduce the following equation:

$$\frac{2\lambda}{2\sin(\theta_{200-\rm m} + \Delta\theta)} = \frac{3\lambda}{2\sin(\theta_{300-\rm m} + \Delta\theta)}, \qquad (5)$$

here the higher order (200) and (300) reflections are preferred because the sensitivity is higher in high angles. Figure 5(a) demonstrates the result of in-plane $\omega/2\theta$ scans from GaN (200) and (300) reflections of the 3 μm-thick sample when the incident angle has been fixed at the total reflection angle of GaN. One can clearly observe an intense peak of GaN (200) and a relative weak GaN (300) diffraction peak. The peak positions are obtained by fitting pseudo-Voigt function to the experimental data. Combining Eq. (5) and Bragg's law, the Bragg angles of GaN are corrected by considering zero setting of instrumental alignment and the in-plane lattice parameter a of subsurface GaN layer is determined as 3.1829 Å±0.0005 Å. In a similar way, the (004) and (006) reflections are performed at the out-of-plane high-resolution XRD setup to directly measure the lattice parameter c.[19]

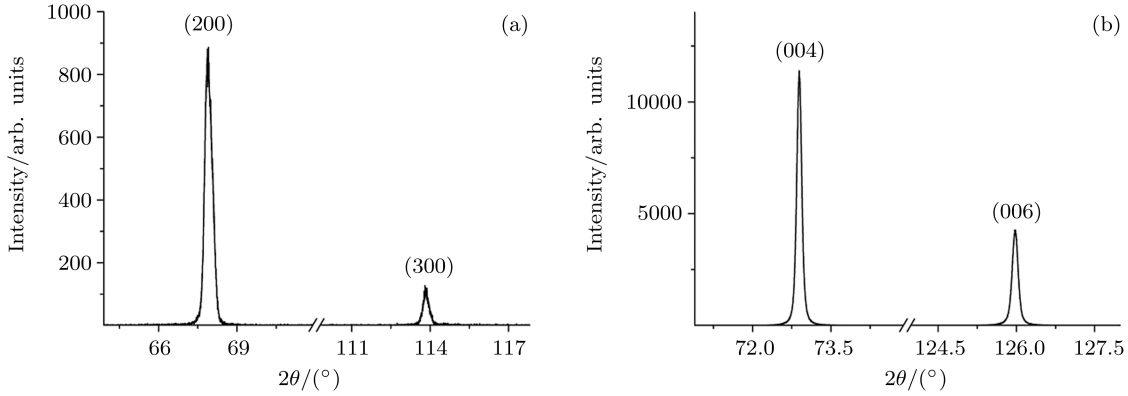


Fig. 5. (a) The XRD $\omega/2\theta$ scan along GaN [100] measured in the in-plane setup and (b) XRD $\omega/2\theta$ scan along GaN [002] measured in the conventional out-of-plane setup.

As seen in Fig. 5(b), the spectrum contains two intense diffraction peaks, (004) and (006), recorded from the same GaN sample and the lattice parameter c is determined to be 5.1901 Å±0.0004 Å by using the following equation:

$$\frac{2\lambda}{2\sin(\theta_{004-\rm m} + \Delta\theta)} = \frac{3\lambda}{2\sin(\theta_{006-\rm m} + \Delta\theta)}. \qquad (6)$$

Based on the method presented above, the lattice parameters a and c of GaN samples are determined and listed in Table 1, where the data of mosaic tilt and twist of these samples are also listed as a reference. The variation in lattice parameters of different samples is attributed to the residual strain presented in GaN epilayers

Table 1. Summary of the main crystallographic parameters in GaN epitaxial films grown on sapphire.

sample	thickness /μm	twist(100) FWHM/(°)	tilt(002) FWHM/(°)	measured a/Å	measured c/Å	calculated a_0/(Å)	calculated c_0/(Å)	ε_a
1	0.6	0.184	0.166	3.1888	5.1860	3.1893	5.1857	–0.00013
2	0.8	0.144	0.113	3.1841	5.1894	3.1892	5.1857	–0.00161
3	1.6	0.117	0.090	3.1831	5.1899	3.1892	5.1856	–0.00191
4	3	0.106	0.066	3.1829	5.1901	3.1892	5.1856	–0.00197

at room temperature. In Fig. 6, the lattice parameter a is plotted versus the lattice parameter c. which can be well characterised by a linear fitting. A linear relationship of the data shows that the GaN samples are dominantly under a biaxial strain field which can be described in terms of isotropic elastic theory.[20] The strain tensor components parallel and perpendicular to the film surface are defined as

$$\varepsilon_a = \frac{a - a_0}{a_0}, \tag{7}$$

$$\varepsilon_c = \frac{c - c_0}{c_0}, \tag{8}$$

where a and c are the measured lattice parameters in GaN epitaxial films and a_0, c_0 are the nominal values for the GaN films in the fully relaxed state. The Poisson's ratio ν is correlated with the ratio between strain along c axis ε_c and in-plane strain ε_a, and in the case of biaxial stress, the relationship is expressed in the following formula:

$$\frac{\varepsilon_c}{\varepsilon_a} = -\frac{2\nu}{1-\nu}. \tag{9}$$

Combining Eqs. (7)–(9) and the lattice parameters a and c measured before, we can determine the unstrained lattice parameters a_0 and c_0, as well as the residual stresses of these GaN films by taking the ratio c_0/a_0 as a constant value. In the calculations, the Poisson's ratio $\nu = 0.18$ is adopted as reported by Moram and Kim,[21,22] which is more suitable for metal-organic chemical vapour deposition (MOCVD) deposited GaN films with moderate dislocation densities and the mean value of c_0/a_0 ratio is taken from Refs. [23]–[26] which is equal to 1.626. As summarised in Table 1, the calculated unstrained lattice parameters a_0, c_0 in four GaN samples show very small variations. By averaging the calculated values, we determine a_0 and c_0 to be 3.1892 Å±0.0003 Å and 5.1856 Å±0.0005 Å, respectively.

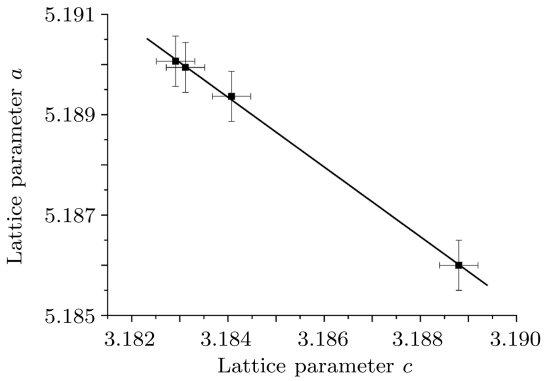


Fig. 6. Plot of in-plane lattice parameter a vs out-of-plane lattice parameter c for GaN samples.

In the case of biaxial strain, the in-plane stress is related to the in-plane strain by the biaxial elastic modulus in terms of the given expression: $\sigma = Y\varepsilon$, where the modulus $Y = c_{11} + c_{12} - 2c_{13}^2/c_{33}$. Taking the biaxial modulus reported by Böttcher *et al.*,[27] the stress state for all studied samples is determined and depicted in Fig. 7. The illustration demonstrates the stress development in the GaN epitaxial films with increasing film thickness. A similar tendency has also be observed by Hearne *et al.* using *in situ* wafer curvature measurement.[28] In-plane stress in GaN heteroepitaxial films at room temperature is considered as a sum of intrinsic and extrinsic stresses and evolves corresponding to 3D–2D transition of the growth mode during the epitaxial growth. At the early stage of growth, an intrinsic tensile stress arises at the point when high-temperature islands of deposited GaN begin to coalesce. The strain is inhomogeneously distributed along the depth and decreases with increasing film thickness within the order of coalescence thickness. An extrinsic compressive stress, on the other hand, builds up during the cooling down process from growth temperature to room temperature due to the mismatch of the thermal expansion coefficients, making an important contribution to the observed compressive stress. On the complete establishment of

2D growth mode, the compound compressive stress reaches a maximum as much as –0.89 Gpa at room temperature. It should be noted that the strain and stress states are often determined by comparing lattice parameters of strained GaN film with unstrained ones of bulk GaN. However, the available data of reference lattice parameters of unstrained GaN are quite scattered, being not very consistent with each other, as summarised by Moram.[16] Furthermore, substantial differences in the GaN lattice parameters

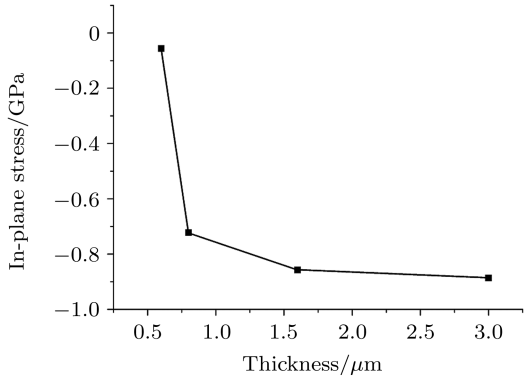


Fig. 7. The in-plane stresses of GaN samples development with increasing layer thickness.

are presented between bulk and homoepitaxial GaN prepared by different fabrication techniques.[29] Therefore, it may make errors during the stress and strain determination. In comparison, the approach employed in this study allows us to evaluate specific values of in-plane stress and unstrained lattice parameter simultaneously without limitation of the reference lattice parameters. Moreover, the approach can also be applied to evaluate the lattice constant and stress state in GaN epitaxial films deposited at different growth stages, including very thin layers.

4. Summary

In summary, the in-plane grazing incidence XRD technique has been shown to be a prominent tool for the investigations of mosaic structure and stress evolution in GaN thin epitaxial films. It provides a more efficient and convenient approach for directly evaluating the mosaic twist or the edge-type threading dislocation density in comparison with the extrapolation methods which is usually employed in out-of-plane XRD measurement. Absolute determination of the in-plane lattice parameters of the GaN layers is also realised. According to the biaxial elasticity theory, the lattice parameters of unstrained GaN films and the strain state are determined simultaneously. It is found that the residual compressive stress increases with the increase of coalescence thickness of GaN film and reaches to –0.89 Gpa corresponding to the establishment of the 2D growth mode.

References

[1] Nakamura S, Senoh N, Iwasa N and Nagahama S I 1995 *Jpn. J. Appl. Phys.* **34** L797
[2] Khan M A, Bhattarai A, Kuznia J N and Olson D T 1993 *Appl. Phys. Lett.* **63** 1214
[3] Nakamura S, Senoh M, Nagahama S, Iwasa N, Yamada T, Matsushita T, Kiyoku H and Sugimoto Y 1996 *Jpn. J. Appl. Phys.* **35** L217
[4] Zhang J M, Zou D S, Xu C, Zhu Y X, Liang T, Da X L and Shen G D 2007 *Chin. Phys.* **16** 1135
[5] Chierchia R, Bottcher T, Heinke H, Einfeldt S, Figge S and Hommel D 2003 *J. Appl. Phys.* **93** 8918
[6] Zhao D G, Jiang D S, Zhu J J, Liu Z S, Zhang S M, Liang J W, Li X, Li X Y and Gong H M 2006 *Appl. Phys. Lett.* **88** 3
[7] Miller E J, Yu E T, Waltereit P and Speck J S 2004 *Appl. Phys. Lett.* **84** 535
[8] Rosner S J, Carr E C, Ludowise M J, Girolami G and Erikson H I 1997 *Appl. Phys. Lett.* **70** 420
[9] Wu Y X, Zhu J J, Zhao D G, Liu Z S, Jiang D S, Zhang S M, Wang Y T, Wang H, Chen G F and Yang H 2009 *Chin. Phys.* B **18** 4413
[10] Chuang S L and Chang C S 1996 *Phys. Rev.* B **54** 2491
[11] Huang C F, Lu C F, Tang T Y, Huang J J and Yang C C 2007 *Appl. Phys. Lett.* **90** 3
[12] Cantu P, Wu F, Waltereit P, Keller S, Romanov A E, DenBaars S P and Speck J S 2005 *J. Appl. Phys.* **97** 10
[13] Ding Z B, Wang Q, Wang K, Wang H, Chen T X, Zhang G Y and Yao S D 2007 *Acta Phys. Sin.* **56** 2873 (in Chinese)
[14] Zhang J C, Zhao D G, Wang J F, Wang Y T, Chen J, Liu J P and Yang H 2004 *J. Cryst. Growth* **268** 24
[15] Dosch H 1987 *Phys. Rev.* B **35** 2137
[16] Moram M A and Vickers M E 2009 *Rep. Prog. Phys.* **72**
[17] Bond W L 1960 *Acta Crystallogr.* **13** 814
[18] Fewster P F and Andrew N L 1998 *Thin Solid Films* **319** 1
[19] Zheng X H, Wang Y T, Feng Z H, Yang H, Chen H, Zhou J M and Liang J W 2003 *J. Cryst. Growth* **250** 345
[20] Kisielowski C, Kruger J, Ruvimov S, Suski T, Ager J W, III, Jones E, Liliental-Weber Z, Rubin M, Weber E R, Bremser M D and Davis R F 1996 *Phys. Rev.* B **54** 17745
[21] Moram M A, Barber Z H and Humphreys C J 2007 *J. Appl. Phys.* **102** 4
[22] Kim K, Lambrecht W R L and Segall B 1996 *Phys. Rev.* B **53** 16310

[23] Harutyunyan V S, Aivazyan A P, Weber E R, Kim Y, Park Y and Subramanya S G 2000 *J. Phys.* D: *Appl. Phys.* **34** A35

[24] Yamaguchi M, Yagi T, Sota T, Deguchi T, Shimada K and Nakamura S 1999 *J. Appl. Phys.* **85** 8502

[25] Detchprohm T, Hiramatsu K, Itoh K and Akasaki I 1992 *Jpn. J. Appl. Phys.* **31** L1454

[26] Balkas C M and Davis R F 1996 *J. Am. Ceram. Soc.* **79** 2309

[27] Böttcher T, Einfeldt S, Figge S, Chierchia R, Heinke H, Hommel D and Speck J S 2001 *Appl. Phys. Lett.* **78** 1976

[28] Hearne S, Chason E, Han J, Floro J A, Figiel J, Hunter J, Amano H and Tsong I S T 1999 *Appl. Phys. Lett.* **74** 356

[29] Darakchieva V, Monemar B and Usui A 2007 *Appl. Phys. Lett.* **91** 3